Microchim Acta (2017) 184:423–429
DOI 10.1007/s00604-016-2023-0

ORIGINAL PAPER

Enhanced amperometric immunoassay for the prostate specific antigen using Pt-Cu hierarchical trigonal bipyramid nanoframes as a label

Lei Jiao[1] · Zonggang Mu[1] · Luyang Miao[1] · Wenwen Du[1] · Qin Wei[1] · He Li[1]

Received: 14 September 2016 / Accepted: 19 November 2016 / Published online: 28 November 2016

Abstract A dual enhancing strategy has been employed to develop a sandwich type of electrochemical immunoassay for the prostate specific antigen (PSA). The signal is enhanced by using Pt-Cu hierarchical trigonal bipyramid nanoframes (HTBNFs) and a composite consisting of Fe_3O_4 nanoparticles and reduced graphene oxide in polydopamine that serve to capture the primary antibody (Ab1). This nanocomposite shows better electrical conductivity than Fe_3O_4 and reduced graphene oxide (RGO), respectively, alone. The Pt-Cu HTBNFs were used to label the secondary antibody (Ab2) and act as tags for signal amplification by virtue of their outstanding electrochemical reduction activity towards H_2O_2. At a working potential of +0.1 V (vs. SCE), the interference by dissolved oxygen can be avoided. This immunoassay is highly sensitive, with a linear range that extends from 0.1 pg·mL^{-1} to 5 ng·mL^{-1} and an ultralow detection limit of 0.03 pg·mL^{-1}.

Keywords Prostate specific antigen · Dual enhancing strategy · Interference by dissolved oxygen · Ultrasensitive detection · Cyclic voltammetry

Lei Jiao and Zonggang Mu contributed equally as co-first author.

Electronic supplementary material The online version of this article (doi:10.1007/s00604-016-2023-0) contains supplementary material, which is available to authorized users.

✉ He Li
lihecd@gmail.com

[1] School of Chemistry and Chemical Engineering, and School of Biological Science and Technology, University of Jinan, Jinan 250022, China

Introduction

The quantitation of biomarkers plays a significant role in early cancer diagnostics and proteomics research, which have attracted remarkable attention in the field of biological sensing [1–5]. However, conventional sensing methods for detection of biomarker like radioimmunoassay [6], enzyme-linked immunosorbent assay [7], chemiluminescent assay [8] and fluorescence assay [9] always need complicated procedure, long response time and expensive cost. There is a need for developing an alternative approach for rapid, quantitative, sensitive and selective detection of biomarkers. Particularly, electrochemical immunoassays have shown great prospects due to their high sensitivity, rapid response, simple instrumentation, and low cost [10]. The signal amplification strategy plays a pivotal role in the development of sensitive electrochemical immunoassay, Especially, enzymes induced signal amplification, which can decompose unique substrates and then yield electron transfer by the corresponding enzymatic reaction, have become the most commonly used strategy for the fabrication of electrochemical immunoassay [11, 12] However, enzyme as a kind of biological molecule is easy to lose activity, which becomes a bottleneck for enzyme induced signal enhancing strategy.

Nanomaterials with high electrocatalytic activity such as noble metal nanoparticles [13] and metal oxide nanoparticles [14] were utilized to develop signal labels, which can maintain the electrocatalytic activity effectively under complicated experimental environments and then significantly improve the detection performance of the electrochemical immunoassay. Among them, noble metal nanoparticles demonstrate enzyme-like activity for highly selective electrochemical reduction of H_2O_2 which can become ideal signal enhancer to improve the sensitivity of electrochemical immunoassay.

The reduction of dissolved oxygen has become an unnegligible factor for affecting the practical application of electrochemical immunoassay, which can occur due to the diffusion of electroactive product generated at one electrode to a neighboring electrode, interfere with the amperometric response [15]. To solve this limits, Lai and his cooperators reported an electrochemical immunoassay using Au-labeled horseradish peroxidase catalytically aniline oxidative polymerization for produced poly-aniline, which can be electrochemical measured at a relatively positive potential (+0.1 V) as working potential to be avoidance of the interference of dissolved oxygen [16].

Here in, we report on a sandwich type electrochemical immunoassay with high sensitivity and selectivity using Pt-Cu HTBNFs as signal enhancer for detection of PSA. It demonstrates a broad linear range (0.1 pg mL^{-1} - 5 ng mL^{-1}) and an ultralow detection limit of 0.03 pg mL^{-1}. Firstly, the prepared Pt-Cu HTBNFs possess big specific surface due to its unique hierarchical trigonal bipyramid nanoframes structure and exhibit superior electrochemical reduction activity towards H_2O_2 because of its large amounts of catalytic active sites which can be attributed to the expose of high-index crystal face. Secondary, Pt-Cu HTBNFs with good biocompatibility can conjugate antibodies easily as signal enhancer by the good affinity between Pt atoms and amino groups of antibodies, which can also enhance the stability and sensitivity of the electrochemical immunoassay. More important, Pt-Cu HTBNFs can cause electrochemical reduction of H_2O_2 from a positive potential. As a consequence, + 0.1 V was selected as working potential resulting the avoidance of the interference of dissolved oxygen. Thereafter, Fe_3O_4-RGO with excellent electronic conductivity as a sensing platform can fast transfer all generated electrochemical reduction currents towards H_2O_2 from Pt-Cu HTBNFs, which can significantly amplify the detection signals of the immunosensors.

Experimental section

Materials and instruments

Graphene oxide (GO) was prepared by Hummers method [17]. Iron dichloride ($FeCl_2{\cdot}4H_2O$), glutaraldehyde and ammonium hydroxide solution ($NH_4{\cdot}OH$) were obtained from Tianjin Fu Yu chemical co., Ltd. (Tianjin China, http://fuyuhuagong.cn.china.cn). Dopamine hydrochloride, hexachloroplatinic acid (H_2PtCl_6), cupric chloride dehydrate ($CuCl_2{\cdot}2H_2O$), potassium iodide (KI), ethylene glycol (EG), polyvinylpyrrolidone (PVP) and bovine serum albumin (BSA) were obtained from Aladdin Industrial Corp (www.aladdin-e.com). Prostate-specific antigen (PSA) and PSA antibody were bought from Shanghai Linc-Bio Co., Ltd. (Shanghai, China, www.linc-bin.cn). Phosphate buffer (PB) was prepared by mixing 0.067 M Na_2HPO_4 and 0.067 M KH_2PO_4 stock solution. Ultrapure water was used throughout the experiments.

A CHI760E electrochemical workstation (Chenhua Instrument Shanghai Co., Ltd., China, www.chinstr.com) was applied into process all electrochemical measurements. The elements of the composites were obtained using Energy Dispersive X-ray Spectroscopy (EDS) (JEOL JSM-6700 F microscope, Japan, www.jeol.co.jp). Transmission electron microscopy (TEM) images were recorded with a Philips CM200 UT (Field Emission Instruments, USA, www.usa.philips.com). The X-ray diffraction (XRD) was conducted from 10^0 to 80^0 (Bruker AXS, Germany, http://bruckgmbh.cn). Fourier transform infrared spectroscopy (FTIR) spectrum was measured by VERTEX 70 spectrometer (Bruker, Germany, http://bruckgmbh.cn). Conventional three-electrode system was used for all electrochemical measurements: a glassy carbon electrode (GCE, 4 mm in diameter) as the working electrode, a platinum wire electrode as the counter electrode and a saturated calomel electrode (SCE) as the reference electrode.

Synthesis of Fe_3O_4-RGO

Fe_3O_4-RGO was synthesized according to previous report [18]. In brief, 30 mg of GO was dispersed in 30 mL of ultrapure water by ultrasonic dispersion for 5 h. Subsequently, 50 mM of $FeCl_2{\cdot}4H_2O$ was adding into the above solution, and the pH value was adjusted between 10 and 11 by adding 30% of $NH_4{\cdot}OH$. This solution was transferred to a Teflon-lined stainless steel autoclave and heated at 180°C for 12 h. The final black color precipitates were washed with ultrapure water and ethanol several times. Finally, the product was dried in a vacuum oven at 70°C overnight.

Synthesis of amino functional Fe_3O_4-RGO and conjugated with Ab_1

Amino functional Fe_3O_4-RGO was synthesized according to previous work with a little modification [19, 20]. In this section, the bidentate bonding of the dopamine to the surface of the Fe_3O_4 via the catechol functionality and amine groups at the outer surface did not bind to Fe_3O_4 surface, which can combine with Ab_1 by the crosslinked action of glutaraldehyde. In brief, 10 mg of Fe_3O_4-RGO was adding into 100 mL of dopamine hydrochloride solution (0.5 M) and sonicated for 1 h. And the mixture was incubated for overnight at 180 rpm. Then the mixture was isolated via centrifuging. Finally, the product (amino functional Fe_3O_4-RGO) (2 mg) was washed and collected by magnet and redispersed in 1 mL PB (pH 7.4) after adding 1 mL of 0.25% glutaraldehyde. Thereafter, the

mixture was separated by magnet after shocked for 12 h and the product was sequentially shocked for 12 h after adding 1 mL 200 ng mL^{-1} Ab_1. Finally, the solution was centrifuged by PB to remove free antibody and the product (Fe_3O_4-RGO-Ab_1) was redispersed in 1 mL PB (pH 7.4) for electrochemical immunoassay. The detail illustration of Fe_3O_4-RGO-Ab_1 was shown in Fig. 1B.

Preparation of Pt-Cu HTBNFs and conjugated with Ab_2

According to Chen's work [21], 1 mL of aqueous $CuCl_2 \cdot 2H_2O$ (20 mM), 1 mL of aqueous $H_2PtCl_6 \cdot 6H_2O$ (20 mM), 0.05 mL of aqueous KI (5 M), 160 mg of PVP, and 10 mL of EG were added in a 20 mL vial at room temperature. After the vial had been capped, the mixture was stirred for around 3 min. The resulting homogeneous mixture was transferred into an oil bath and heated at 140°C for 90 min before it was cooled to room temperature. The products were collected by centrifugation at 10000 rpm for 10 min, and then washed with ethanol-acetone mixture twice. The pure Pt nanoparticles were prepared with similarly Pt-Cu HTBNFs without the precursor of $CuCl_2 \cdot 2H_2O$.

In previous work, Pt nanoparticles can conjugate with antibodies due to its good affinity between Pt atom and amino group of antibodies [22]. 2.0 mg of Pt-Cu HTBNFs was dispersed in 1 mL of 200 ng mL^{-1} of Ab_2, and then the mixture was shocked 12 h at 4°C. Next, the product (Pt-Cu-Ab_2) was washed with PB (pH 7.4) in consecutive centrifugation to remove free antibody and then passivated with 1% BSA for another 1 h. The final product (Pt-Cu-Ab_2) was redispersed in 1 mL of PB (pH 7.4) and stored at 4°C until used. Figure 1A given the detail illustration of Pt-Cu-Ab_2.

Fabrication of the electrochemical immunoassay

The electrochemical immunoassay was established by the procedure as illustrated in Fig. 1C. In brief, a GCE (glassy carbon electrode) was polished with alumina slurry to obtain a mirror-like surface and dried at room temperature. Subsequently, 6 μL of Fe_3O_4-RGO-Ab_1 was put on the surface of GCE and incubated for 1 h. Furthermore, 3 μL of BSA (1%) was put onto surface of the electrode coating Fe_3O_4-RGO-Ab_1 for incubation of 0.5 h to block non-specific sites. After that, pH 7.4 of PB was used to wash the surface of electrode to remove excess BSA. Afterwards, 6 μL of different concentration of PSA was dropped onto the electrode decorated BSA/ Fe_3O_4-RGO-Ab_1 by the specific reaction between antibody and antigen for incubating 1 h at 37°C. Then, 6 μL of Pt-Cu-Ab_2 was dropped onto the electrode surface for incubating another 1 h and washed with pH 7.4 of PB for twice to remove unbonded Pt-Cu-Ab_2. Finally, the developed electrochemical immunoassay was ready for PSA detection.

Electrochemical detection by electrochemical immunoassay

The electrodes were measured by a CHI760E electrochemical workstation. The cyclic voltammetry was operated from −0.6 V to 0.6 V (scan rate: 100 mv s^{-1}). The amperometry was operated at +0.1 V and the method of electrochemical impedance spectroscopy (EIS) operated at an open-circuit voltage as to 0.20 V and the frequencies were scanned from 1 Hz to 100,000 Hz. At the progress of electrochemical detection, Pt-Cu HTBNFs can catalyze H_2O_2 to H_2O, which induced electron transfer at the electrode surface. The current responses can reflect the concentration of PSA. Hence, the electrochemical immunoassay can be applied into electrochemical detection of PSA.

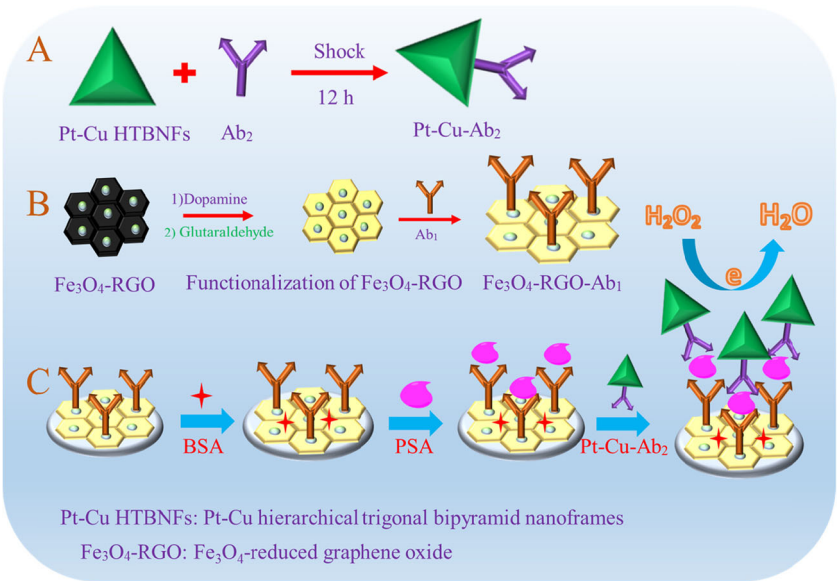

Fig. 1 Illustration the fabrication process of the electrochemical immunoassay

Results and discussion

Choice of materials

To improve the sensitivity and stability of the electrochemical immunoassay, Fe_3O_4-RGO was selected as substrate material for coating antibody due to its good electronic conductivity and easy surface functionalization. The synergistic effect between the Fe_3O_4 and RGO of Fe_3O_4-RGO results in the better electronic conductivity than Fe_3O_4 and RGO alone. On the other hand, amine groups can be induced by the bidentate bonding of the dopamine to the surface of the Fe_3O_4 via the catechol functionality, which is easily for coating antibody via crosslinked action of glutaraldehyde. Furthermore, Fe_3O_4-RGO was synthesized by skillfully one-pot hydrothermal process without complicated fabrication procedures. The detail mechanism of synthesized Fe_3O_4-RGO was shown as follows:

$$2Fe^{2+} + GO \rightarrow 2\ Fe^{3+} + RGO$$
$$2\,Fe^{3+} + Fe^{2+} + 8\,OH^- \rightarrow Fe_3O_4 + 4\,H_2O$$
$$3Fe^{3+} + GO(8OH^-) \rightarrow Fe_3O_4 + 4H_2O + RGO$$

As a consequence, Fe_3O_4-RGO can be a kind of ideal substrate material for establishing an ultrasensitive electrochemical immunoassay. It is clear to see that Fe_3O_4 nanoparticles were loaded on the graphene surface by the TEM image (Figure S1) and the inset figure indicated that Fe_3O_4-RGO had good magnetic response which was in favor of developing magnetic electrode. As shown in Figure S2, the black line was the FTIR spectra of GO. It is easy to see the characteristic peaks located at 1249, 1615, 1744, and 3400 cm^{-1} corresponding the stretching vibrations of epoxy (C–O), C = C, carboxylic (C = O) and hydroxyl group, which was fitted well with the observation of previous work [17]. The blue line was the FTIR spectra of Fe_3O_4. Obviously, the strong peak at 579 cm^{-1} was attributed to the lattice adsorption of iron oxide (Fe-O), which was similar to the reported observation [18]. The red line was the FTIR spectra of Fe_3O_4-RGO. Obviously, the peaks of epoxy and carboxylic were disappeared which indicated that GO was reduced by Fe^{2+} to obtain the Fe_3O_4-RGO nanocomposites successfully. The XRD pattern of Fe_3O_4-RGO nanocomposites was shown in Figure S3. A face centered cubic structure for the Fe_3O_4 loaded on the surface of graphene was obtained (JCPDS 88–0866). The diffraction peak for reduced graphene was at around 26.4°, which was similar to the reported result [23]. Figure 2a was the cyclic voltammetry curves (CVs) of bare GCE (black line), Fe_3O_4 (blue line), reduced graphene oxide (rGO) (red line) and Fe_3O_4-RGO (green line) in 0.1 M KCl solution containing 5.0 mM potassium ferricyanide solution. It was explicit that the CVs of GCE and all modified electrodes were given a well-defined reversible redox behavior of $[Fe(CN)_6]^{3-/4-}$. Fe_3O_4-RGO modified electrode had the best conductivity owing to the obtained biggest redox peak current, which can enhance the sensitivity of the immunosensor.

Pt-Cu HTBNFs were selected as label materials, which were depended on its stronger electrochemical reduction activity towards H_2O_2 and excellent biocompatibility. Pt atom can coat antibodies by the bonding of Pt-NH_2 [22], which need not complicated molecular recognition procedures. As shown by the TEM image in Figure S4, Pt-Cu HTBNFs emerged a trigonal bipyramid nanoframe structure with good biocompatibility (inset: the Pt-Cu HTBNFs dispersion in PB at different time). The porous nanoframes possessed large surface area which can supply many active catalytic sites for electrochemical reduction of H_2O_2. The XRD spectrum of Pt-Cu HTBNFs was indexed as a face-centered cubic

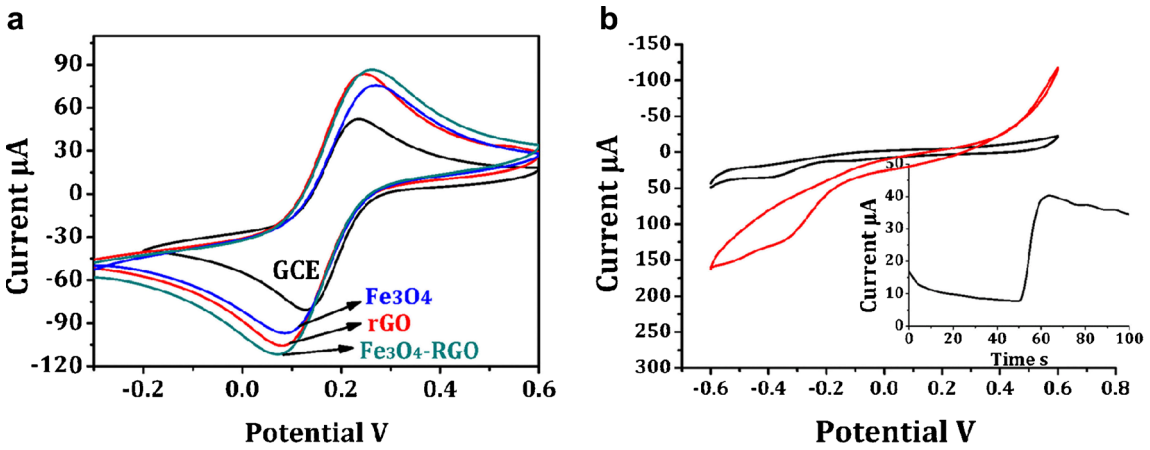

Fig. 2 **a** Cyclic voltammetry curves of bare GCE (*black line*), Fe_3O_4 (*blue line*), rGO (*red line*), Fe_3O_4-RGO (*green line*) in 0.1 M KCl solution containing 5.0 mM potassium ferricyanide solution; **b** The cyclic voltammetry curves of the electrode modified with 2 mg mL^{-1} Pt-Cu HTBNFs in pH 7.4 PB without H_2O_2 (*black line*), and with 5 mM H_2O_2 (*red line*), inset (The i-t curves of the electrode modified with 2 mg mL^{-1} Pt-Cu HTBNFs under 0.1 V in pH 7.4 PB)

structure, which lies between pure Pt (JCPDS 04–0802) and Cu (JCPDS 04–0836) (Figure S5). This result was fitted well with the previous observation [21]. The exposure of high-index facets can improve the catalytic efficiency. The EDS gave evidences for the presence of Pt and Cu elements in this alloy with the atomic percent of Pt and Cu were 17.9% and 82.1%, respectively (Figure S6). As expected, after adding H_2O_2, the reduction current towards H_2O_2 of Pt-Cu alloy HTBNFs modified electrode increased significantly, which meant that Pt-Cu HTBNFs had outstanding electrocatalytic performance. (Fig. 2b). Especially, in order to be avoidance of interference of dissolved oxygen, +0.1 V was selected to as working potential and the satisfied current changes at +0.1 V was obtained, which can be observed by i-t curves of Pt-Cu HTBNFs modified electrode at +0.1 V (Fig. 2b **inset**).

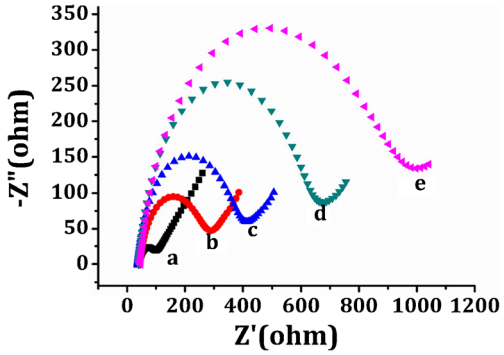

Fig. 4 EIS of electrodes in 0.1 M KCl solution containing 5.0 mM $Fe(CN)_6^{3-}$/ $Fe(CN)_6^{4-}$ (1:1): GCE (**a**), Fe_3O_4-RGO-Ab_1/GCE (**b**), BSA/Fe_3O_4-RGO-Ab_1/GCE (**c**), PSA/BSA/Fe_3O_4-RGO-Ab_1/GCE (**d**) and Pt-Cu-Ab_2/PSA/BSA/Fe_3O_4-RGO-Ab_1/GCE (**e**)

Characterization of the signal amplification strategy of electrochemical immunoassay

To evaluate the dual signal amplification strategy of the electrochemical immunoassay, the substrate materials and the label materials were used to detection of PSA (1 ng mL^{-1}) with the same experimental conditions. As expected, compared with other substrate materials (RGO and Fe_3O_4), the Fe_3O_4-RGO gave the largest current response, which can enhance the sensitivity of electrochemical immunoassay (Fig. 3a). As shown in Fig. 3b, compared with pure Pt nanoparticles, Pt-Cu HTBNFs were obtained the higher current response due to its porous nanoframe structures, large specific surface area and synergistic effect between Pt and Cu, which can improve the electrochemical reduction activity towards H_2O_2 and load much more antibodies to enhance the sensitivity of the electrochemical immunoassay.

Characterization of the assembly of electrochemical immunoassay

Electrochemical impedance spectroscopy (EIS) is an important tool for characterization of the assembly process of electrochemical immunoassay. The impedance spectroscopy consists of two parts: semicircle and linear portion. The semicircle portion at higher frequencies corresponds to electron-transfer-limited process and the diameter of semicircle portion equals resistance of the electrode surface. The linear portion at lower frequencies represents the diffusion-limited process [24]. Figure 4 shows the Nyquist diagrams of the electrodes modified with different materials. It was clear to observe resistance changed significantly. Resistance of the electrodes modified with GCE (curve a), Fe_3O_4-RGO-Ab_1/GCE (curve b) BSA/Fe_3O_4-RGO-Ab_1/GCE (curve c), PSA/BSA/Fe_3O_4-RGO-Ab_1/GCE (curve d) and Pt-Cu-Ab_2/PSA/BSA/ Fe_3O_4-RGO-Ab_1/GCE (curve e) were increased one by one, indicating the electrodes modified successfully.

Optimization of conditions

The following parameters were optimized: (A) concentration of Fe_3O_4-RGO; (B) concentration of Pt-Cu HTBNFs; (C) sample pH value; (D) concentration of H_2O_2. Respective data and Figures are given in the Electronic Supporting Material (Figure S7). We found the following experimental conditions

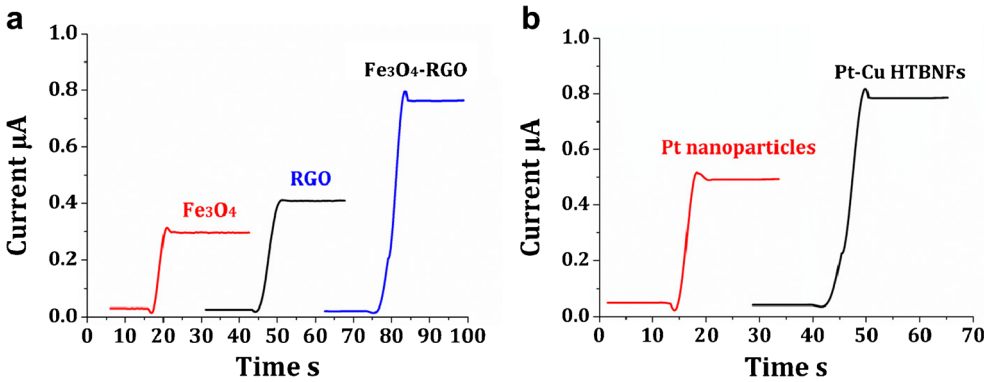

Fig. 3 The current responses of electrochemical immunoassay with **a** different substrate materials; **b** different label materials

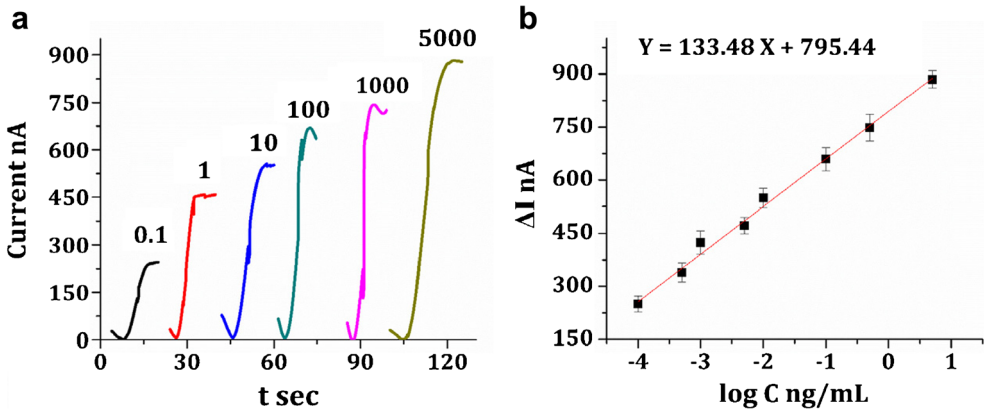

Fig. 5 Current responses of the electrochemical immunoassay for the varied concentration of PSA(0.1, 1, 10, 100, 1000, 5000 pg mL^{-1}) under 5 mM H_2O_2 at 0.1 V (**a**); Calibration curve of the immunosensor toward PSA under 5 mM H_2O_2 at 0.1 V (**b**) from 0.1 pg mL^{-1} to 5 ng mL^{-1}, error bar = RSD (n = 5)

to give best results: (A) concentration of Fe_3O_4-RGO of 2.0 mg L^{-1}; (B) concentration of Pt-Cu HTBNFs of 2.0 mg L^{-1}; (C) sample pH value of 7.4; (D) concentration of H_2O_2 of 5 mM.

Analytical detection

Under the optimal experimental conditions, the developed electrochemical immunoassay was used to detect PSA. As shown in Fig. 5a, it was current responses of the electrochemical immunoassay for the varied concentration of PSA under 5 mM H_2O_2 at 0.1 V. It can be seen that the current response values were increased gradually following the increase of PSA concentration. Accordingly, a calibration curve for PSA was obtained (Fig. 5b). Obviously, the regression equation of the calibration curve can be expressed as: ΔI (nA) = 133.48 log C (ng mL^{-1}) + 795.44 (R^2 = 0.98). The electrochemical immunoassay presents a broad linear detection range of 0.1 pg mL^{-1} ~ 5 ng mL^{-1} and a low detection limit of 0.03 pg mL^{-1} (S/N = 3). Additionally, as compared with other methods in Table S1, this work exhibited more sensitive performance towards PSA detection.

Selectivity, stability and reproducibility

To examine the selectivity of the electrochemical immunoassay, interfering substances (100 ng mL^{-1}): bovine serum albumin (BSA), carbohydrate antigen 125 (CA-125), carcinoembryonic antigen (CEA) and alpha fetoprotein (AFP) were assayed by the developed immunosensor, respectively (Figure S8). The relative standard deviations (RSD) of the electrochemical immunoassay were less than 2%, which indicated the satisfactory selectivity of the electrochemical immunoassay. Additionally, under the confidence interval of 95%, the significance values of the four paired samples were 0.942, 0.915, 0.184 and 0.205, respectively, which were larger than 0.05 (Table S2). This observation shows that there was no statistical significance which meant the good selectivity of the immunosensor.

The stability of the electrochemical immunoassay was periodically measured towards 1 ng mL^{-1} of PSA (Figure S9A). The generated current response can maintain around 92% of the fresh value after 5 weeks storage, suggesting the acceptable stability for this immunosensor. Besides, a series of five electrodes were all employed to assay 1 ng mL^{-1} of PSA (Figure S9B). The RSD of the detection were less than 3.5%, indicating that the offered immunosensor had favorable reproducibility.

Standard addition method was put into use for detecting the recovery of different concentrations of PSA to evaluate the feasibility of the electrochemical immunoassay. As depicted in Table S3, the recovery was in the range of 98.0%–103%, revealed that the immunosensor had good potential for clinical analysis of PSA.

Conclusion

A dual amplification strategy has been employed to fabricate the immunosensor, which is based on amino functionalization of Fe_3O_4-reduced graphene oxide nanocomposites for biomolecular immobilization and the Pt-Cu hierarchical trigonal bipyramid nanoframes as label enhancer. Especially, +0.1 V as working potential can be avoidance of interference of dissolved of oxygen. Owing to the resulted ultrasensitive and reliable detection performance, the developed electrochemical immunoassay shows a large potential for clinical applications.

Acknowledgements This work was partially supported by the National Natural Science Foundation of China (no. 21245007 and 81000976).

Compliance with ethical standards The author(s) declare that they have no competing interests.

References

1. Uludag Y, Köktürk G (2015) Determination of prostate-specific antigen in serum samples using gold nanoparticle based amplification and lab-on-a-chip based amperometric detection. Microchim Acta 182(9–10):1685–1691

2. Yang J, Wen W, Zhang X, Wang S (2015) Electrochemical immunoassay for the prostate specific antigen detection based on carbon nanotube and gold nanoparticle amplification strategy. Microchim Acta 182(9):1855–1861
3. Xu H, Xu Y, Luo X (2015) Peptide-based biosensor for the prostate-specific antigen using magnetic particle-bound invertase and a personal glucose meter for readout. Microchim Acta 182(9–10):93–94
4. Wang Y, Qu Y, Liu G, Hou X, Huang Y, Wu W, Wu K, Li C (2015) Electrochemical immunoassay for the prostate specific antigen using a reduced graphene oxide functionalized with a high molecular-weight silk peptide. Microchim Acta 182(11–12): 2061–2067
5. Peng J, Zhu YD, Li XH, Jiang LP, Abdel-Halim ES, Zhu JJ (2014) Electrochemical immunoassay for the prostate specific antigen using ceria mesoporous nanospheres. Microchim Acta 181(13–14):1505–1512
6. Sloan JH, Ackermann BJ, O'Dell M, Bowsher RR, Dean RA, Konrad RJ (2011) Development of a novel radioimmunoassay to detect autoantibodies to amyloid beta peptides in the presence of a cross-reactive therapeutic antibody. J Pharm Biomed Anal 56(5): 1029–1034
7. Werner MT, Faeste CK, Egaas E (2007) Quantitative sandwich ELISA for the determination of tropomyosin from crustaceans in foods. J Agric Food Chem 55(20):8025–8032
8. Zong C, Wu J, Liu M, Yang L, Liu L, Yan F, Ju H (2014) Proximity hybridization-triggered signal switch for homogeneous chemiluminescent bioanalysis. Anal Chem 86(11):5573–5578
9. Ahn J, Shin YB, Lee JJ, Kim MG (2015) Human alpha-fetal protein immunoassay using fluorescence suppression with fluorescent-bead/antibody conjugate and enzymatic reaction. Biosens Bioelectron 71:115–120
10. Wei Y, Yan L, Li N, Zhang Y, Yan T, Ma H, Wei Q (2015) Sandwich-type electrochemical immunoassay for the detection of AFP based on Pd octahedral and APTES-M-CeO2-GS as signal labels. Biosens Bioelectron 79:482–487
11. Dutta G, Park S, Singh A, Seo J, Kim S, Yang H, Chem A (2015) Low-Interference Washing-Free Electrochemical immunoassay Using Glycerol-3-phosphate Dehydrogenase as an Enzyme Label. Anal Chem 87(7):3574–3578
12. Yan Z, Zheng Y, Kong R, Lian X, Qu F (2016) Ultrasensitive electrochemical immunoassay based on horseradish peroxidase (HRP)-loaded silica-poly(acrylic acid) brushes for protein biomarker detection. Biosens Bioelectron 75:383–388
13. Liu Y, Wang H, Xiong C, Yuan Y, Chai Y, Yuan R (2016) A sensitive electrochemiluminescence immunosensor based on luminophore capped Pd@Au core-shell nanoparticles as signal tracers and ferrocenyl compounds as signal enhancers. Biosens Bioelectron 81:334–340
14. Feng T, Qiao X, Wang H, Zhao S, Hong C (2015) A sandwich-type electrochemical immunoassay for carcinoembryonic antigen based on signal amplification strategy of optimized ferrocene functionalized Fe3O4@SiO2 as labels. Radiat Phys Chem 50(4):24–30
15. Lai G, Jie W, Ju H, Feng Y (2011) Streptavidin-Functionalized Silver-Nanoparticle-Enriched Carbon Nanotube Tag for Ultrasensitive Multiplexed Detection of Tumor Markers. Adv Funct Mater 21(15):2938–2943
16. Lai G, Zhang H, Tamanna T, Yu A (2014) Ultrasensitive immunoassay based on electrochemical measurement of enzymatically produced polyaniline. Anal Chem 86(3):1789–1793
17. Marcano DC, Kosynkin DV, Berlin JM, Sinitskii A, Sun Z, Slesarev A, Alemany LB, Lu W, Tour JM (2010) Improved synthesis of graphene oxide. ACS Nano 4(8):4806–4814
18. Bharath G, Madhu R, Chen SM, Veeramani V, Mangalaraj D, Ponpandian N (2015) Solvent-free mechanochemical synthesis of graphene oxide and Fe3O4–reduced graphene oxide nanocomposites for sensitive detection of nitrite. J Mater Chem A 3(30):15529–15539
19. Li H, Wei Q, Wang G, Yang M, Qu F, Qian Z (2011) Electrochemical immunoassays for cancer biomarker with signal amplification based on ferrocene functionalized iron oxide nanoparticles. Biosens Bioelectron 26(8):3590–3595
20. An P, Zuo F, Wu YP, Zhang JH, Zheng ZH, Ding XB, Peng YX (2012) Fast synthesis of dopamine-coated Fe3O4 nanoparticles through ligand-exchange method. Chin Chem Lett 23(9):1099–1102
21. Chen S, Su H, Wang Y, Wu W, Zeng J (2014) Size-Controlled Synthesis of Platinum–Copper Hierarchical Trigonal Bipyramid Nanoframes. Angew Chem Int Ed 127(1):110–115
22. Wei Q, Zhao Y, Du B, Wu D, Cai Y, Mao K, Li H, Xu C (2011) Nanoporous PtRu Alloy Enhanced Nonenzymatic Immunosensor for Ultrasensitive Detection of Microcystin-LR. Adv Funct Mater 21(21):4193–4198
23. Shen J, Hu Y, Shi M, Lu X, Qin C, Li C, Ye M (2009) Fast and Facile Preparation of Graphene Oxide and Reduced Graphene Oxide Nanoplatelets. Chem Mater 21(15):3514–3520
24. Liu Y, Ma H, Gao J, Wu D, Ren X, Yan T, Pang X, Wei Q (2016) Ultrasensitive electrochemical immunoassay for SCCA detection based on ternary Pt/PdCu nanocube anchored on three-dimensional graphene framework for signal amplification. Biosens Bioelectron 79:71–78